Plasma etching of SiO_2 using remote-type pin-to-plate dielectric barrier discharge

Jae Beom Park,[1] Se Jin Kyung,[2] and Geun Young Yeom[1,2,3,a)]
[1]*SKKU Advanced Institute of Nano Technology (SAINT), Sungkyunkwan University, Suwon, Kyunggi-do 440-746, Republic of Korea*
[2]*Department of Advanced Materials Science and Engineering, Sungkyunkwan University, Suwon, Kyunggi-do 440-746, Republic of Korea*
[3]*The National Program for Tera-Level Nanodevice, Hawolgok-dong, Sungbuk-ku, Seoul 136-791, Republic of Korea*

(Received 4 March 2008; accepted 25 August 2008; published online 24 October 2008)

Atmospheric pressure plasma etching of SiO_2 was examined using a modified remote-type dielectric barrier discharge (DBD), called "pin-to-plate DBD." The effect of adding four gases CF_4, C_4F_8, O_2, and Ar to the base gas mixture containing N_2 (60 slm) (slm denotes standard liters per minute)/NF_3 (600 SCCM) (SCCM denotes cubic centimeter per minute at STP) on the SiO_2 etch characteristics was investigated. The results showed that the SiO_2 etch rate decreased continuously with increasing C_4F_8 (200–800 SCCM) addition, whereas the SiO_2 etch rate increased with increasing CF_4 (1–10 slm) addition up to 7 slm CF_4. This increase in the SiO_2 etch rate up to 7 slm CF_4 was attributed to the effective removal of Si in SiO_2 by F atoms through the removal of oxygen in SiO_2 by carbon in the CF_X in the plasma. However, the decrease in SiO_2 etch rate with further increases in CF_4 flow rate above 7 slm was attributed to the formation of a thick C–F polymer layer on the SiO_2 surface. A SiO_2 etch rate of approximately 243 nm/min was obtained with a gas mixture of N_2 (60 slm)/NF_3 (600 SCCM)/CF_4 (7 slm), and an input voltage and operating frequency to the source of 10 kV and 30 kHz, respectively. The addition of 200 SCCM Ar to the above gas mixture increased the SiO_2 etch rate to approximately 263 nm/min. This is possibly due to the increased ionization and dissociation of reactive species through penning ionization of Ar. © *2008 American Institute of Physics*. [DOI: 10.1063/1.2999645]

I. INTRODUCTION

Plasma processing is used in the production of flat panel display devices such as indium tin oxide etching and the deposition and etching of thin film transistor materials (SiO_2, amorphous silicon, and Si_3N_4). Plasma processing for flat panel displays is generally operated at low pressure. However, various plasma processing techniques operating at atmospheric pressure are attracting considerable attention for the next generation of flat panel display devices due to the extremely large area of the flat panel display substrate and the need for in-line processing.[1–3]

Various atmospheric pressure plasma sources have been reported with each claiming of low running cost, low gas temperature, wide applicability to surface treatment, cleaning, etching, and thin film deposition. Several atmospheric pressure plasma sources have been studied for such processing, including the radio frequency plasma torch, dielectric barrier discharge (DBD), microwave discharge, and pulsed corona plasma.[4–6] Among the various atmospheric pressure plasma sources, DBD has received a great deal of attention for its potential industrial applications such as plasma ashing, etching, and thin film deposition. DBD, which consists of two parallel electrodes covered by dielectric plates, has been studied most widely due to the easier generation of a stable glow discharge and the possibility of larger area plasma processing. However, arcing occurs frequently during DBD operation and can damage the substrate during processing, which has limited the use of DBD. In addition, conventional DBD sources have a low processing rate due to the low plasma density. Thermal damage can also occur due to the direct contact of the plasma with the substrate. Some of the above disadvantages can be overcome using a remote-type plasma DBD source, which avoids radiation damage to the substrate from the plasma because the remote plasma does not come in direct contact with the substrate. An additional benefit is the increased control of the radical flux.[7–9]

This study examined plasma etching of SiO_2 for applications to the next generation of flat panel display processing using a modified remote-type pin-to-plate DBD at atmospheric pressure. Pin-to-plate DBD has been used to increase the processing rate by increasing the plasma density.[10] The effect of additive gases on the SiO_2 etch characteristics was investigated by adding the fluorocarbon gases and O_2 (or Ar) in the base N_2/NF_3 gas mixture.

II. EXPERIMENTAL DETAILS

Figure 1 shows a schematic of the remote-type plasma pin-to-plate DBD system used in the experiment. The discharge source consisted of a multipin power electrode and a blank ground electrode located vertically above the substrate. The aluminum electrodes were 50×300 mm^2 in size. The power electrode was machined to have multipins, as shown

a)Electronic mail: gyyeom@skku.edu. Tel.: +82-31-299-6562. FAX: +82-31-299-6565.

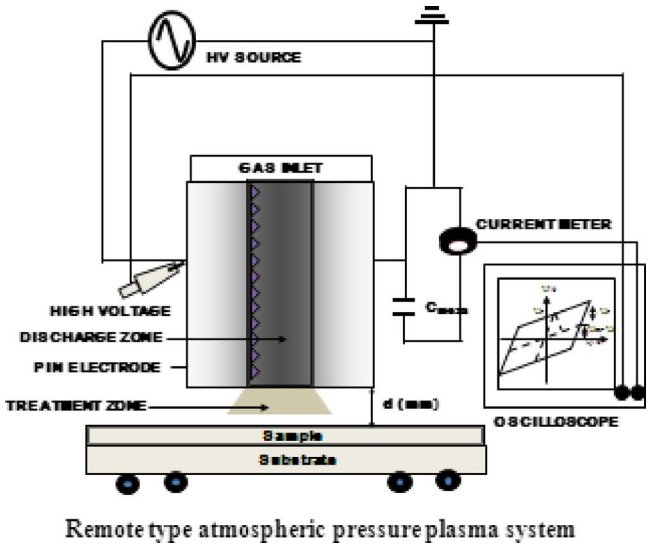

FIG. 1. (Color online) Schematic of the remote-type atmospheric pressure discharge system (pin-to-plate DBD) used in the experiment.

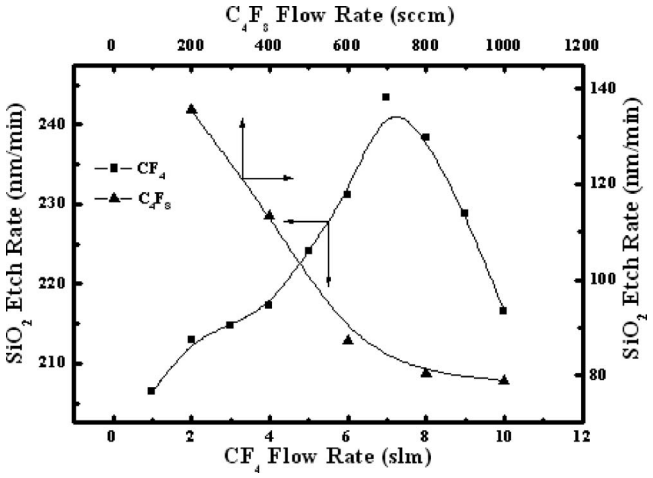

FIG. 2. Effect of the additive gas flow rate (CF_4: 1–10 slm, C_4F_8: 200–1000 SCCM) to the base N_2 (60 slm)/NF_3 (600 SCCM) gas mixture on the SiO_2 etch rate. The input voltage was 10 kV and the frequency was 30 kHz.

in Fig. 1, and both electrodes were coated with alumina. The power electrode was connected to an ac (alternative current) power supply with a frequency range of 20–30 kHz and a maximum power of 4 kW. The input voltage to the power electrode was maintained at 10 kV (rms voltage) in order to ensure stable and uniform plasma while the ac frequency was fixed at 30 kHz. The etching gas consisted of a base gas mixture of N_2 (60 slm)/NF_3 (600 SCCM) with CF_4 (or C_4F_8) and O_2 (or Ar). The SiO_2 sample was located 2 mm below the remote-type DBD source. The remote-type plasma DBD system was installed in a plastic box to remove the etch products and control the impurities. The residual gas was removed using an exhaust fan.

The SiO_2 etching rate was estimated by measuring the etching depth with a step profilometer (TENCOR, alpha-step 500 with a 5 nm uncertainty of the etch step measurement). Optical emission spectroscopy (OES) (PCM 420 SC-Technology) was used to measure the optical emission intensity of the species in order to detect radicals or activated species in the plasma. Accurate and reliable measurements of the excited species could not be achieved due to the weak OES signals from the treatment zone (Fig. 1). Therefore, in order to observe the excited species, the OES signals from the discharge zone in Fig. 1 were measured instead. The chemistry of the etched oxide surface was examined by x-ray photoelectron spectroscopy (XPS) (Thermo VG SIGMA PROBE).

III. RESULTS AND DISCUSSION

Figure 2 shows the SiO_2 etch rate as a function of the CF_4 and C_4F_8 flow rate in the base N_2/NF_3 gas mixture at a rms voltage and frequency of 10 kV and 30 kHz. The CF_4 and C_4F_8 flow rates were varied from 1 to 10 slm and 200 to 1000 SCCM, respectively. As shown in the figure, the SiO_2 etch rate increased with increasing CF_4 flow rate to a maximum of approximately 243 nm/min at 7 slm CF_4 but the etch rate decreased significantly with further increases in CF_4 flow rate. The SiO_2 etch rate decreased almost linearly with increasing C_4F_8 gas concentration in the base N_2/NF_3 gas mixture from 200 to 1000 SCCM. Indeed, during low-pressure plasma etching, SiO_2 is not etched easily unless the Si–O bonds are broken by energetic ion bombardment. However, in these experiments, the SiO_2 etching that was obtained without ion bombardment using a remote-type plasma DBD with N_2/NF_3 was attributed to the enhanced chemical reactions of SiO_2 with reactive gas radicals as a result of surface heating during exposure to the atmospheric pressure plasma. However, surface heating cannot explain the difference in etch rate between the etching gases containing either CF_4 or C_4F_8. Therefore, the plasma chemistry during etching and the etched SiO_2 surface were examined by OES and XPS, respectively, in order to explain the difference in SiO_2 etch rate with the addition of CF_4 and C_4F_8.

Figure 3(a) shows the OES data of the remote-type pin-to-plate DBD for the N_2/NF_3-generated plasma and when 7 slm of CF_4 and 600 SCCM of C_4F_8 were added separately to the base N_2/NF_3 gas composition. The wavelengths examined ranged from 210 to 290 nm. The input voltage and operating ac frequency of the discharges were maintained at the same levels as those shown in Fig. 2. As shown in the figure, various peaks were observed in the wavelength range investigated. Of these peaks, the peaks at 245–250 nm and 268–275 nm were used to estimate the CF and CF_2 peak intensities, respectively.[11] Despite the significantly lower C_4F_8 flow rate than CF_4, the CF, and CF_2 peak intensities in the plasma generated with 600 SCCM C_4F_8 were comparable to those generated with 7 slm CF_4. Very small peak intensities were also observed for CF and CF_2 in the plasma generated by the base N_2/NF_3 gas mixture, which may be due to either the recombination of fluorine and residual carbon in the gas phase or the presence of residual CF_x on the walls of the remote plasma source during repeated operation.

Figures 3(b) and 3(c) show the relative OES peak intensities of F, CF, and CF_2 as a function of the CF_4 (1–10 slm) and C_4F_8 (200–1000 sccm) flow rates, respectively. An optical emission peak for the F atom was observed at 704.5 nm.[12] As shown in Fig. 3(a), the OES peak intensities for CF

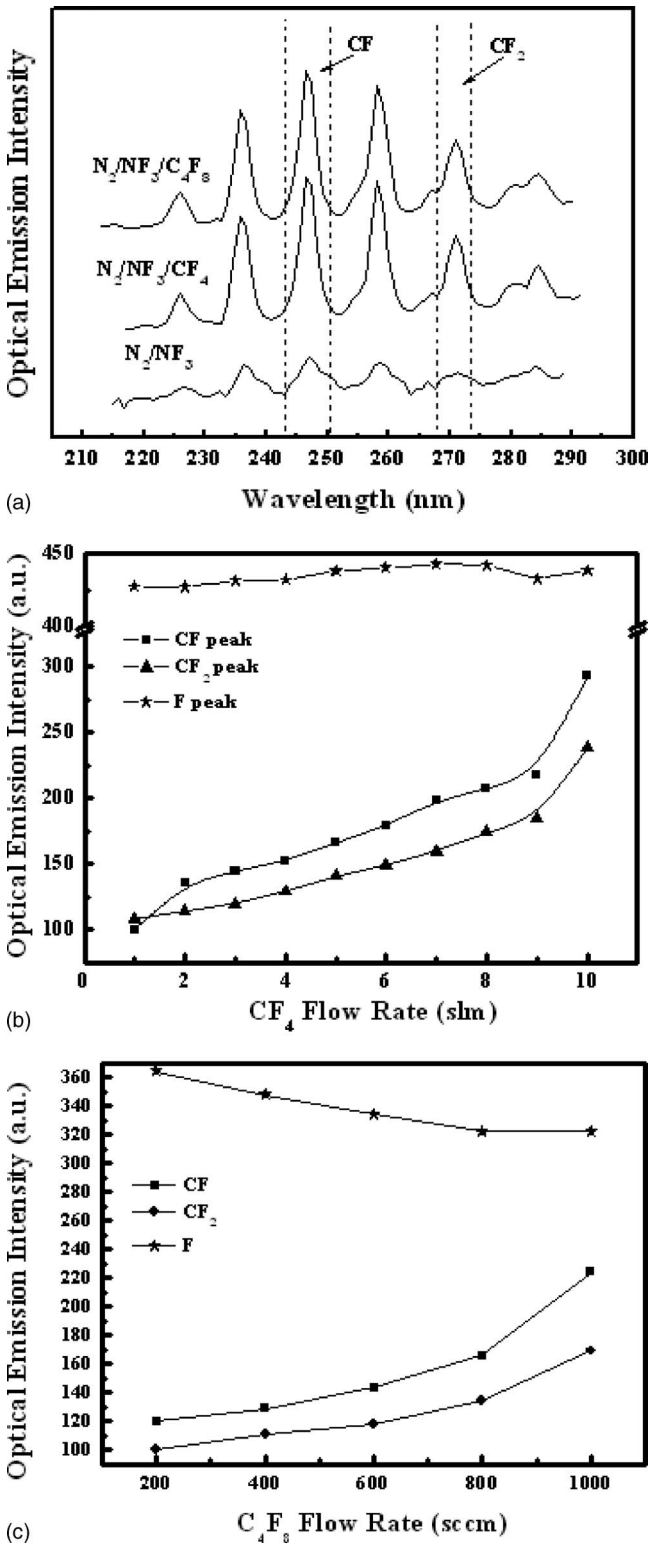

FIG. 3. (a) OES spectrum obtained from the plasma generated with the base N_2 (60 slm)/NF_3 (600 SCCM) gas mixture and CF_4 (7 slm) or C_4F_8 (600 SCCM) addition. OES peak intensities of F, CF, and CF_2 measured as a function of (b) CF_4 and (c) C_4F_8 flow rates in the base N_2/NF_3 gas mixture. The input voltage was 10 kV and the operating frequency was 30 kHz.

and CF_2 increased almost linearly with increasing CF_4 flow rate due to the higher carbon-related gas flow rate in the gas mixture. However, the optical emission intensity of F increased only slightly with increasing CF_4 flow rate up to 7 slm and decreased slightly with further increases in CF_4 flow rate. Therefore, the overall effect of the CF_4 flow rate on the OES peak intensity of F was not significant. When C_4F_8 was added, the OES peak intensities for CF and CF_2 also increased with increasing C_4F_8 flow rate in a similar manner to that observed with CF_4. However, the OES intensity of F decreased almost linearly with increasing C_4F_8 flow rate. This was attributed to the recombination of F with carbon in C_4F_8 due to the low F/C ratio of C_4F_8.

The increase in SiO_2 etch rate observed with increasing CF_4 flow rate up to 7 slm in the base N_2/NF_3 gas mixture was attributed to the removal of oxygen from the SiO_2 by CF_X ($x=1,2$) in the plasma, which reduces the level of Si removal in SiO_2 through the formation of volatile SiF_X ($x=1-4$). However, a large increase in CF_X ($x=1,2$) in the plasma, >7 slm, appeared to induce the formation of a C–F polymer layer on the SiO_2 surface and prevent a reaction between F and Si,[13–15] which decreased the SiO_2 etch rate. In the case of SiO_2 etching with C_4F_8, although the increased level of CF_X ($x=1,2$) in the plasma due to the addition of a small amount of C_4F_8 may have removed the oxygen in SiO_2 in a similar manner to that observed with CF_4 addition, the significant decrease in F with increasing C_4F_8 flow rate appeared to negate this effect by decreasing the SiO_2 etch rate. In addition, the level of SiO_2 etching was reduced by the formation of a C–F polymer layer on the SiO_2 surface at the higher C_4F_8 flow rate.

In order to understand the SiO_2 etching behavior, the C 1*s* binding states in the x-ray photoelectron spectrum of the SiO_2 surface etched in the remote-type pin-to-plate DBD system with the base N_2/NF_3 gas combination and the gas containing added CF_4 or C_4F_8 were examined as a function of the CF_4 [3–9 slm, Fig. 4(a)] and C_4F_8 [200–800 SCCM, Fig. 4(b)] flow rates. The voltage to the source was 10 kV and the operating frequency was 30 kHz. The SiO_2 etching time prior to XPS analysis was maintained at 1 min in order to examine the C–F polymer layer formed on the etched SiO_2 surface. As shown in Figs. 4(a) and 4(b), C–C bonding was observed at 284.5 eV while C–F and C$-F_2$ bondings were observed at 289.5 and 291.5 eV respectively.[16] As shown in Fig. 4(a), the C–F and C$-F_2$ bonding peaks increased with increasing CF_4 flow rate in the gas mixture. However, these peak intensities were not significantly high until 7 slm CF_4. When the CF_4 flow rate was increased to 9 slm, there was a significant increase in the bonding peak intensities related to C–F and C$-F_2$. Therefore, the increased SiO_2 etch rate with increasing CF_4 flow rate up to 7 slm was attributed to the effective etching of SiO_2 due to oxygen and Si removal in SiO_2 by the carbon in CF_X and F in the plasma. On the other hand, the C–F polymer layer did not prevent SiO_2 etching due to its thinness. When the CF_4 flow rate was increased to more than 7 slm, as shown in the XPS data, a thick C–F polymer layer was formed as a result of the high CF_X ($x=1,2$) flow rate in the plasma, which decreased the SiO_2 etch rate significantly. In the case of the SiO_2 surface etched by C_4F_8, as shown in Fig. 4(b), the bonding peak intensities of C–C, C–F, and C$-F_2$ increased slowly with increasing C_4F_8 flow rate, even though the peak related to the C$-F_X$ polymer was similar to that observed at 9 slm CF_4. Therefore, it is believed that the decrease in SiO_2 etch rate with increasing

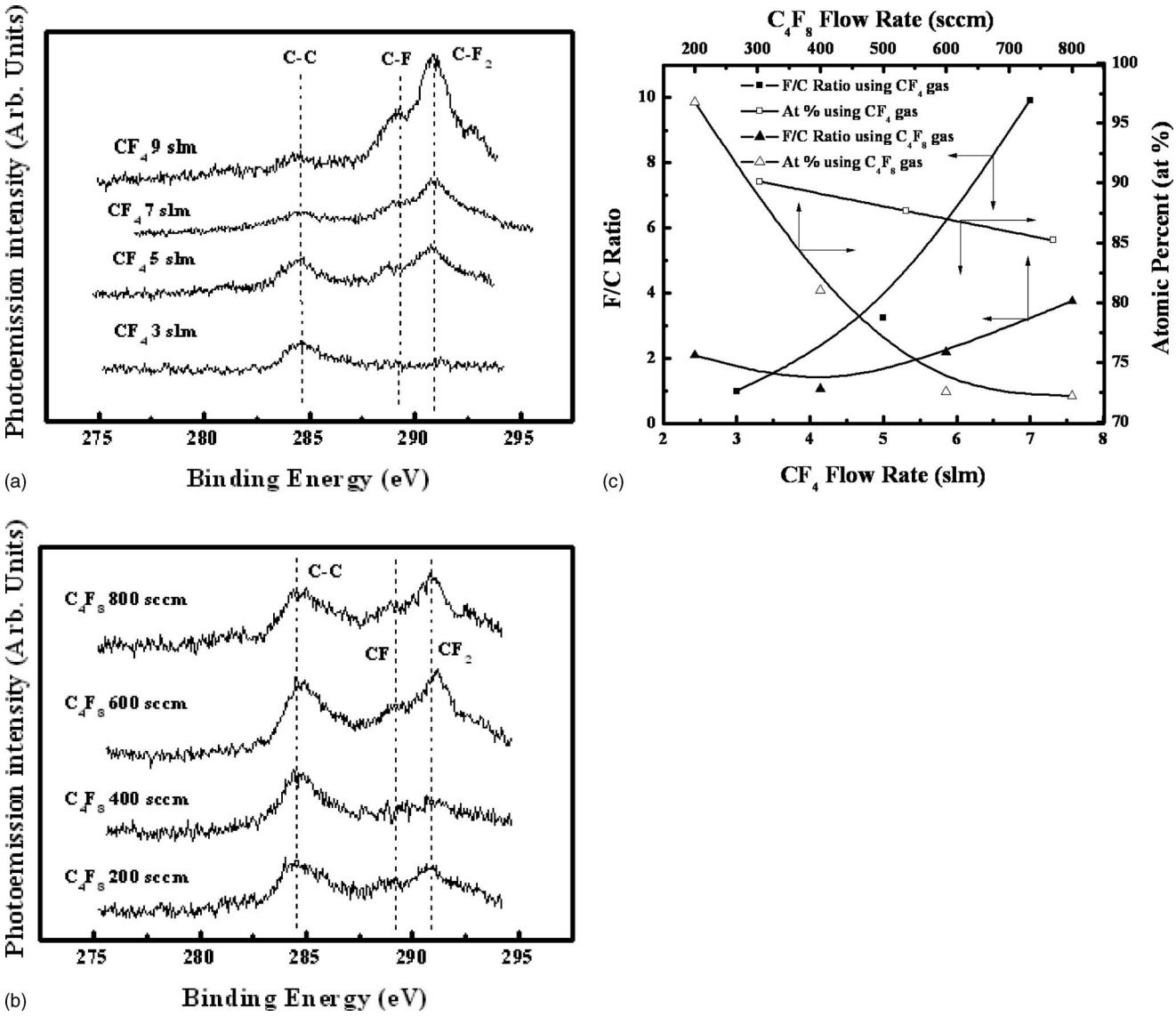

FIG. 4. C 1*s* XPS spectra of the SiO_2 surface after etching with (a) N_2 (60 slm)/NF_3 (600 SCCM)/CF_4 (3–9 slm) and (b) N_2 (60 slm)/NF_3 (600 SCCM)/C_4F_8 (200–800 SCCM). (c) The atomic percentage of the Si 2*p* XPS peak of the SiO_2 surface after etching and the F/C ratios of the C–F polymer layer on the SiO_2 surface after etching with N_2 (60 slm)/NF_3 (600 SCCM)/CF_4 (3–7 slm) and N_2 (60 slm)/NF_3 (600 SCCM)/C_4F_8 (200–800 SCCM).

C_4F_8 flow rate was related more to the decreased F density in the plasma, which was due to F removal by the formation of CF_X ($x=1-3$) with dissociated C_4F_8 in the plasma, than to the formation of a thick C–F polymer layer, particularly at low C_4F_8 flow rates.

The thickness of the C–F polymer layer can be evaluated qualitatively by measuring the change in the atomic percentage of the Si 2*p* or O 1*s* XPS peaks before and after etching as well as by considering the attenuation of the signals through the C–F polymer layer. Therefore, the atomic percentage of Si on the etched SiO_2 surface was measured as a function of the CF_4 (3–7 slm) and C_4F_8 (200–800 SCCM) flow rates. The results are shown in Fig. 4(c). The F/C ratios of the C–F polymer were estimated by the equation $(F/C=(I_{CF}+2I_{CF_2}+3I_{CF_3})/\Sigma I_C)$ using the XPS C 1*s* data in Figs. 4(a) and 4(b) for the CF_4 and C_4F_8 flow rates, respectively. The atomic percentage of Si 2*p* decreased with increasing CF_4 flow rate, indicating an increase in the C–F polymer layer thickness. However, the atomic percentage of Si 2*p* was >85% until the CF_4 flow rate reached 7 slm, indicating that no significant C–F polymer layer had formed on the SiO_2 surface during etching with CF_4 up to 7 slm. The atomic percentage of Si at low C_4F_8 flow rates was similar to that at 7 slm CF_4, indicating the formation of a thin C–F polymer layer. However, the atomic percentage decreased to 70% as the C_4F_8 flow rate was increased to 800 SCCM, indicating the formation of a thick C–F polymer layer. In addition, the F/C ratios of the C–F polymer layer were generally lower for the etching gas containing C_4F_8 addition than those containing CF_4. This suggests that the decrease in the SiO_2 etch rate with increasing C_4F_8 flow rate is related to the lower F density in the plasma at low C_4F_8 flow rates due to the thinness of the C–F polymer layer, as shown in Fig. 3(c) as well as to both the decreased F density in the plasma and increased C–F polymer layer thickness at high C_4F_8 flow rates. Moreover, the change in SiO_2 etching with increasing CF_4 flow rate was believed to be more affected by the F

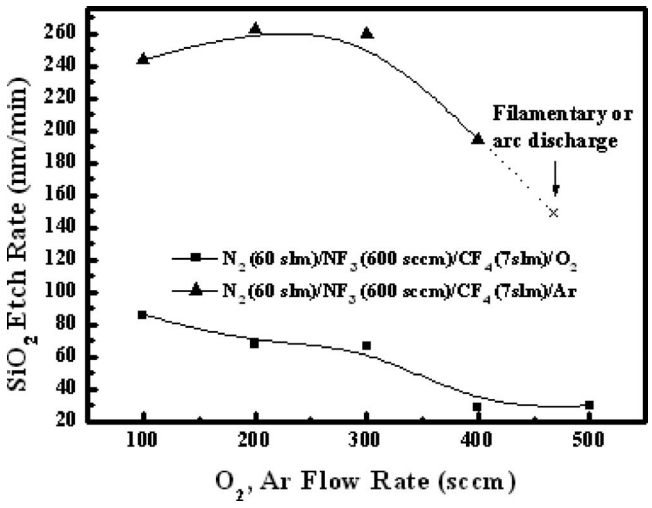

FIG. 5. SiO_2 etch rate as a function of the additive gases (O_2 or Ar) to the optimized gas composition of N_2 (60 slm)/ NF_3 (600 SCCM)/CF_4 (7 slm). The input voltage was 10 kV and the operating frequency was 30 kHz.

atomic density in the plasma due to the formation of a thin C–F polymer layer on the SiO_2 surface during etching with CF_4.

In order to further investigate the possible increase in the SiO_2 etch rate, O_2 and Ar gases were added to the optimized N_2 (60 slm)/NF_3 (600 SCCM)/CF_4 (7 slm) gas mixture in the range of 100–500 SCCM, and the effect on the SiO_2 etch rate was examined. The results are shown in Fig. 5. The input voltage and operating frequency to the source were 10 kV and 30 kHz, respectively. As shown in the figure, the SiO_2 etch rate decreased significantly with increasing O_2 flow rate in the optimized $N_2/NF_3/CF_4$ gas mixture. On the other hand, it increased slightly from 243 nm/min to 263 nm/min with increasing Ar flow rate up to 200 SCCM but decreased with further increases in Ar flow rate. Although the addition of O_2 to the optimized $N_2/NF_3/CF_4$ gas mixture decreased the level of C–F polymer layer formation on the SiO_2 surface due to the formation of filamentary discharges by O_2 addition, the plasma density and SiO_2 etch rate decreased significantly with increasing O_2 flow rate. The slight increase in SiO_2 etch rate with increasing Ar flow rate up to 200 SCCM was attributed to the increase in ionization and further dissociation of the reactive species as a result of the penning ionization effect of Ar caused by collisions between metastable Ar and the reactive molecules.[17] However, a further increase in the Ar flow rate beyond 200 SCCM also induced a filamentary discharge that decreased the SiO_2 etch rate.

IV. CONCLUSIONS

This study examined the plasma etching of SiO_2 at atmospheric pressure using a remote-type pin-to-plate DBD with gas mixtures of $N_2/NF_3/CF_4$ or C_4F_8 as a function of the CF_4 and C_4F_8 flow rates. The SiO_2 etch rate increased with increasing CF_4 flow rate up to 7 slm but decreased with further increases in CF_4 flow rate. However, the SiO_2 etch rate decreased continuously with increasing C_4F_8 flow rate. The increased SiO_2 etch rate with increasing CF_4 flow rate up to 7 slm was attributed to the effective removal of Si in SiO_2 by F through the removal of oxygen in SiO_2 by the carbon in CF_X ($x=1,2$). This is because the C–F polymer layer that formed on the SiO_2 surface was not thick enough to prevent SiO_2 etching. However, the decrease in SiO_2 etch rate with increasing CF_4 flow rate above 7 slm was attributed to the formation of a thick C–F polymer layer on the SiO_2 surface, which prevented the reaction between the reactive species and SiO_2. The steady decrease in SiO_2 etch rate with increasing C_4F_8 flow rate was attributed to the decrease in F atomic density in the plasma due to the recombination of F with the carbon from the dissociated C_4F_8 because there was no significantly thick C–F polymer layer observed on the etched SiO_2 surface. The addition of O_2 to the optimized gas mixture of N_2 (60 slm)/NF_3 (600 SCCM)/CF_4 (7 slm) decreased the SiO_2 etch rate due to the formation of a filamentary discharge. However, the addition of up to 200 SCCM Ar to the optimized gas mixture increased the SiO_2 etch rate, possibly due to the increased ionization and dissociation of the plasma as a result of the penning ionization effect of Ar. However, the SiO_2 etch rate decreased with further increases in Ar flow rate above 200 SCCM.

ACKNOWLEDGMENTS

This work was supported by the National Program for Tera-Level Nanodevices of the Korea Ministry of Science and Technology as a 21st Century Frontier Program.

[1] S. Okazaki, M. Kogoma, M. Uehara, and Y. Kimura, J. Phys. D **26**, 889 (1993).
[2] T. Yokoyama, M. Kogoma, S. Kanazawa, T. Moriwaki, and S. Okazaki, J. Phys. D **23**, 374 (1990).
[3] T. Yokoyama, M. Kogoma, T. Moriwaki, and S. Okazaki, J. Phys. D **23**, 1125 (1990).
[4] C. Tendero, C. Tixier, P. Tristant, J. Desmaison, and P. Leprince, Spectrochim. Acta, Part B **61**, 2 (2006).
[5] E. E. Kunhardt, IEEE Trans. Plasma Sci. **28**, 189 (2000).
[6] A. Schutze, J. Y. Jeong, S. E. Babayan, J. Y. Park, G. S. Selwyn, and R. F. Hicks, IEEE Trans. Plasma Sci. **26**, 1685 (1998).
[7] G. R. Nowling, S. E. Babayan, V. Jankovic, and R. F. Hicks, Plasma Sources Sci. Technol. **11**, 97 (2002).
[8] M. J. Kushner, J. Appl. Phys. **71**, 4173 (1992).
[9] B. E. E. Kastenmeier, P. J. Matsuo, J. G. Langan, and G. S. Oehrlein, J. Vac. Sci. Technol. A **16**, 2047 (1998).
[10] Y. H. Lee, S. J. Kyung, C. H. Jeong, and G. Y. Yeom, Jpn. J. Appl. Phys., Part 2 **44**, L78 (2004).
[11] T. Nakano and K. Yanagita, Jpn. J. Appl. Phys., Part 1 **42**, 663 (2003).
[12] R. Payling and P. Larkins, *Optical Emission Lines of the Elements* (Wiley, Chichester, 2004).
[13] D. Zhang and M. J. Kushner, J. Vac. Sci. Technol. A **19**, 524 (2001).
[14] J. Feldsien, D. S. Kim, and D. J. Economou, Thin Solid Films **374**, 311 (2000).
[15] F. Gaboriau, G. Cartry, M. C. Peignon, and C. Cardinaud, J. Phys. D **39**, 1830 (2006).
[16] J. F. Moulder, W. F. Stickle, P. E. Sobol, and K. D. Bomben, *Handbook of X-Ray Photoelectron Spectroscopy* (Perkin-Elmer, Eden Prairie, MN, 1992).
[17] F. Massines, P. Ségurb, N. Gherardi, C. Khamphan, and A. Ricard, Surf. Coat. Technol. **174-175**, 8 (2003).